EXPERIMENTAL APPARATUS
CONSTRUCTION AND OPERATION

STATUS REPORT OF THE 4π DETECTOR PROJECT

J. van der Plicht, G.D. Westfall, J.E. Yurkon, L. Morris, R. Burleigh, M. Maier, S. Tanaka

We have built and successfully tested a prototype detector for the 4π array planned for operation during NSCL's phase 2. A report of tests and experiments regarding this prototype can be found elsewhere in this Annual Report. The final detector array consists of 30 detector modules, each consisting of a Low-Pressure Multiwire Proportional Counter for heavy fragments, a Bragg Curve Counter for intermediate energy fragments and scintillator telescopes for light particles. The 32 modules (2 for beam entrance and exit) are stacked as a truncated icosahedron or soccerball, and is envisioned in Fig. 1.

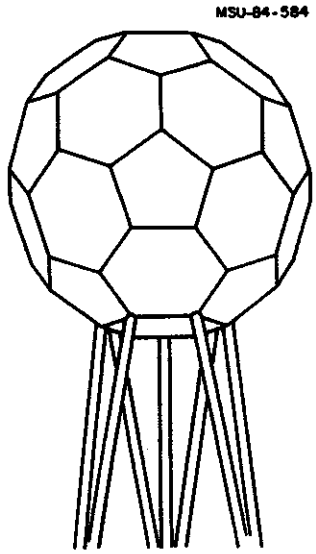

Fig. 1 The Multi-Detector Array, consisting of 20 hexagons and 12 pentagons.

The detectors for the final 4π array will have modifications from the prototype. The walls of the gascounters (both the MWPC and the BCC) will be only 0.125" thick, which allows a solid angle coverage of about 90% of 4π. The cables for signals and voltages will be laid in grooves (0.031" deep) in these frames. The gas lines will be hidden in the corners of the BCC's and scintillators. Design - and detailing work on the detectors is finished.

The scintillator detectors will be completely different from the prototype ones, which consisted of a CaF_2/plastic telescope. A new, slow plastic has been developed by Bicron very recently. Our final 4π array will consist of telescopes of slow plastic as ΔE - and fast plastic as E detector. The advantages of the slow plastic as compared with CaF_2 are:

1. Much easier to machine than CaF_2 in the desired shapes (conical hexagons and pentagons).
2. Same index of refraction for both elements in the telescope.
3. The thin ΔE detector is the fast one (as opposed to the CaF_2/fast plastic system) defining a better electronic trigger signal.

The properties of the plastics discussed are compared in Table 1.

TABLE 1. Properties of three scintillator materials

	fast plastic BC412	slow plastic BC444	CaF2
density (g/cm3)	1.032	1.032	3.19
peak emission (nm)	434	428	435
decay constant (ns)	3.3	180	940
refraction index	1.58	1.58	1.44
light yield (%anthracene)	60	41	100

We tested a "fast/slow" scintillator telescope consisting of a 0.25" thick slow plastic (BC444) as ΔE and a 2" thick fast plastic (BC412) as E. We detected particles produced from the reaction $^{12}C + ^{197}Au$ at 30 MeV/A. The gate width for the fast component was 40 ns, and for the slow component 1 μs. Fig. 2 shows the two-dimensional ΔE vs. E plot. Light particles from protons through alphas were observed and are identified clearly. The peak to background ratio for the protons was about 500 to 1. As for the protons, the particles that "punch through" are also visible.

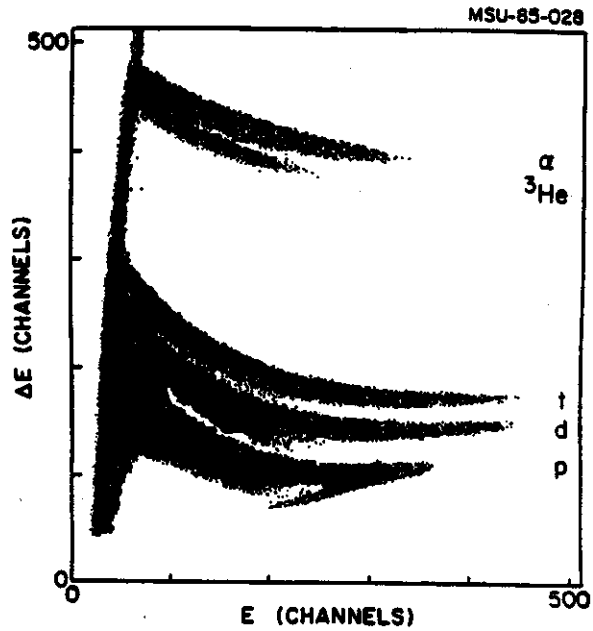

Fig. 2 Particle identification spectrum for a "fast/slow" scintillator phoswich telescope.

The detector modules will be mounted on hexagonally and pentagonally shaped plates. They can be adjusted in position to provide exact alignment. The plates will be mounted on a skeleton structure, thereby providing the vaccumvessel. The whole detector will be able to rotate around the beamaxis to provide access to all elements for the purpose of taking individual modules in and out. This module handling will be done by a specially designed "stuffer".

A laser system is being developed for calibration purposes of the scintillators. Each subarray will be connected to a laser located outside the chamber with fiberoptics cable - and feedthrough. Photodiodes located at the back end of the lightguides will provide stabilization of the laser output.

The data taking electronics plan for the 4π array has been designed. For the 30 MWPC's the 30 BCC's and the 170 Phoswiches we need 550 ADC - and 260 TDC channels. We are planning to utilize the Lecroy (EC Line) FERA system.

THE PROTOTYPE DETECTOR FOR THE 4π ARRAY

G.D. Westfall, J.E. Yurkon, J. van der Plicht, Z.M. Koenig, B.V. Jacak, R. Fox, G.M. Crawley, M.R. Maier, B.E. Hasselquist, R.S. Tickle[a] and D. Horn[b]

A low pressure Multi-Wire Proportional Counter (MWPC), a Bragg Curve Counter (BCC), and an array of CaF_2/plastic scintillator telescopes have been developed in a geometry suitable for close packing into a 4π detector designed to study nucleus-nucleus reactions at NSCL phase 2 energies (up to 200 MeV/nucleon). They form together a "logarithmic detector" for fission fragments (MWPC), intermediate fragments (BCC) and light particles (scintillators). The geometry of the prototype subarray is a truncated hexagonal pyramid and is shown schematically in Fig. 1. The final 4π array will consist of 32 elements, consisting of 20 hexagons (as shown in Fig.1) and 10 pentagons.

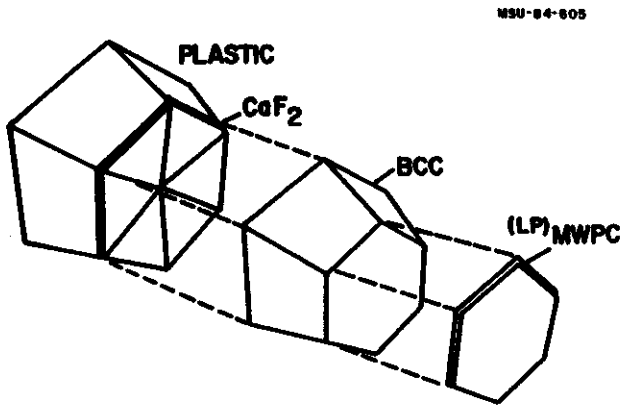

Fig.1 - Schematic representation of one of the 30 subarrays that will make up the multiparticle array.

The remaining 2 pentagons will be used for beam entrance and exit. Together they are packed in a object known as truncated icosahedron (or soccerball) - see Fig.2.

The MWPC is a low pressure gas detector utilizing the double amplification process as discovered by Breskin et. al.[1] This detector forms the inner layer of the 4π array. The total thickness of the detector is 1.6 cm. The distance from target to center of front of the MWPC

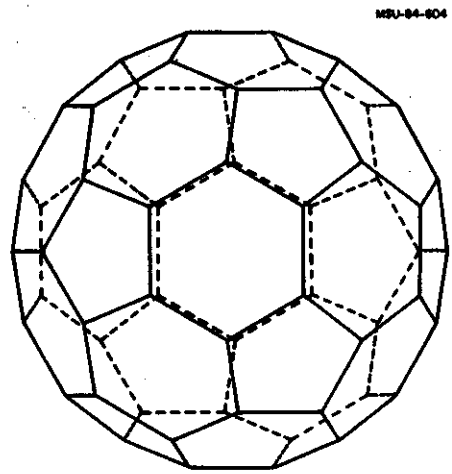

Fig.2 - A 32 face truncated icosahedron, consisting of 20 hexagons and 12 pentagons.

is 15 cm; the solid angle subtended is about 300 msr. The detector is shown in exploded view in Fig. 3. The anode is a plane in the center of the detector composed of gold plated tungsten wires 12 μm in diameter spaced 1 mm apart. These wires are connected to the high voltage and also provide a fast timing signal. The two cathodes are at ground potential and are located 3.2 mm from the wire plane. Each cathode plane consists of a polypropylene foil,stretched to a thickness of about 75 $\mu g/cm^2$. The cathode foils are coated with a resistive strip of Nichrome (Nickel/Chrome 80/20 %). This NiCr strip in turn is coated with 5 mm wide Al strips perpendicular to the NiCr strip as indicated in Fig. 3. The resistance between the end contacts of the cathode foils is typically in the range of 1 - 5 kΩ. The orientation of one striped cathode (say X) is 90^0 with respect to the second (Y). From each cathode, the position is calculated by the data-acquisition computer with the charge division method, i.e. X=L/(L+R) and Y=U/(U+D). Here L,R,U,D symbolize the left,right,up and down signals.

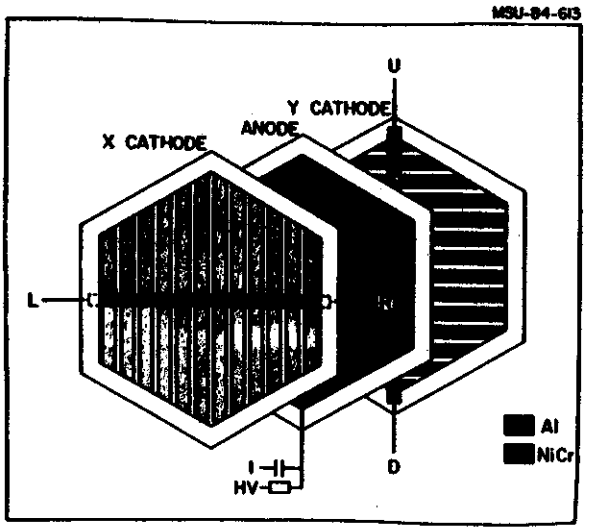

Fig.3 - Exploded view of the hexagonal MWPC.

The pressure window is also a 75 $\mu g/cm^2$ stretched polypropylene foil supported by three stainless steel wires across the entrance of the detector. The MWPC is designed to operate at a pressure of 2 torr isobutane gas.

A Bragg curve counter (BCC) is basically an ionization chamber with its field parallel to the incoming particles[2]. In this way the range of the particles that are stopped in the detector can be measured. The BCC takes advantage of the fact that the maximum specific ionization of a stopping ion is proportional to the atomic number of the particle. By measuring the maximum of the ionization one obtains the charge Z of the particle; the integral of the ionization is a measure of the energy E. The electrons liberated by the ionization of the stopping charged particle drift to an anode which is shielded by a Frisch grid. Since the electric field is parallel to the path of the particle, one measures the charge collected on the anode as a function of time, and thus obtains the complete energy loss distribution of the stopping ion. In the present counter the range of subtended angles to be covered is very large and the information concerning the ionization of the stopping particles will be lost if the electrons do not drift parallel to the trajectory of the particle. Thus, a field shaping grid was installed inside the BCC to approximate a radial field. This is illustrated in Fig. 4. The design of this field shaping grid was calculated with the program POISSON in cylindrical geometry. The main structure of the BCC is a hexagonal pyramid made from 6.35 mm G10 fiberglass epoxy laminate. The length of the BCC is 15 cm; the entrance window of the BCC has a minor diameter of 10 cm. The pressure window of the BCC is made of 6 μm (or 800 $\mu g/cm^2$) thick aluminized mylar supported by a wire grid with 1 cm spacing. The distance between the cathode and the Frisch grid is 14 cm. The Frisch grid is made of 12.5 μm gold plated tungsten wires with a 0.5 mm spacing. The anode is a similar wire grid located 1 cm behind the Frisch grid. The rear pressure window is formed by the scintillator telescopes. The BCC usually operates at a pressure of 500 torr Ar/CH_4 (90/10%) gas.

The scintillator telescopes are designed to detect light particles from pions to alphas. The basic technique for obtaining ΔE and E information for particle identification and energy measurement is a "phoswich" technique[3]. This technique takes advantage of the different time constants for the emission of scintillation light from CaF_2 crystals and from plastic scintillators. We used 3 mm thick CaF_2(Eu) crystals for the ΔE scintillator, and 15 cm thick BC412 plastic scintillator for the E. The characteristic time for light emission from CaF_2 is 1 μsec while plastic scintillators emit most

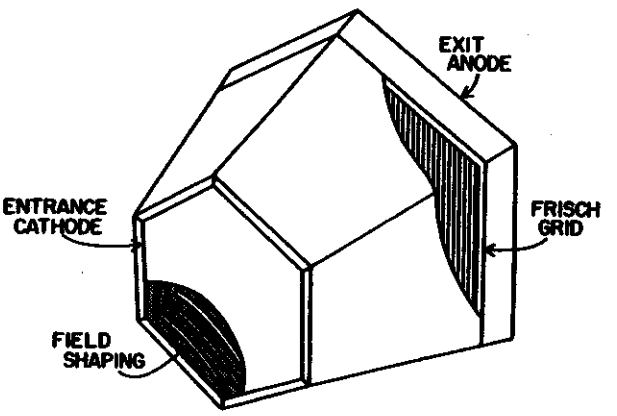

Fig.4 - Schematic view of the Bragg Curve Counter.

of their light in 50 nsec. Thus one can obtain the energy loss in a thin CaF_2 ΔE detector by putting a long, delayed gate on the output signal of the phototube while the energy deposited in the plastic scintillator is obtained using a prompt, short gate.

The 6 scintillator telescopes are each connected via lightguides to Philips XP2202 photomultipliers. The light emission of CaF_2 is about the same as that for anthracene, and that of the plastic (BC412), about 60 % of anthracene.

The detector elements of the prototype array have been tested extensively, both with radioactive sources (where possible) and with heavy-ion beams. Experiments were performed with beams of 360 MeV ^{12}C and 490 MeV ^{14}N at the National Superconducting Cyclotron Laboratory of Michigan State University, with 230 MeV ^{35}Cl at the Tandem/Linac accelerator of Argonne National Laboratory, and with 4 GeV ^{40}Ar at the Bevalac of Lawrence Berkeley Laboratory.

We present here tests of the MWPC as performed with a $^{252}Cf(sf)$ source. A two-dimensional plot of X - position versus Y - position is shown in Fig. 5. The plot shows the detector, exposed to fission fragments from the ^{252}Cf source through a mask. The mask consists of a hexagon, covering the whole of the detector except an outer rim of about 1.5 mm and a lettering pattern. We concluded that the position resolution of the hexagonal MWPC in both dimensions is better than 1 mm FWHM. The right part of the plot appears more compressed than the left part. This is due to a non - uniform evaporation of the NiCr strip on this cathode foil, causing a change in resistance going from one end to the other.

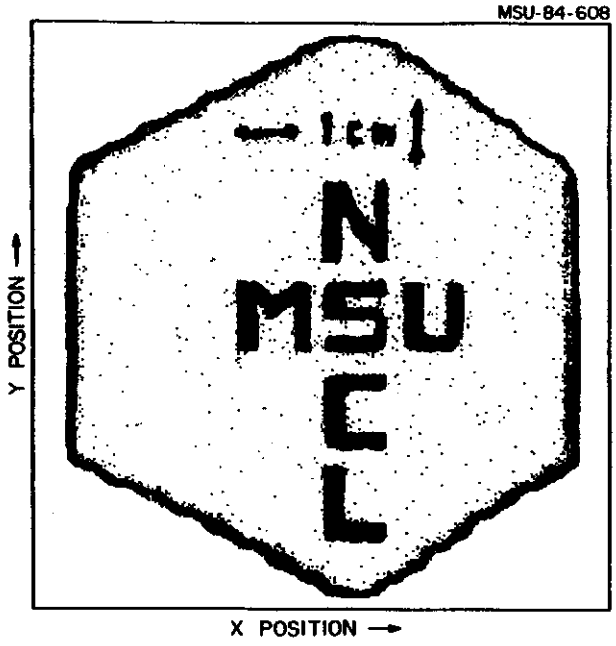

Fig.5 - Contour plot of a two - dimensional MWPC position spectrum, showing horizontal (X - axis) versus vertical (Y - axis) position.

The Bragg Curve Counter can be read out using two different techniques. Firstly, from the measured Bragg curve the peak amplitude and the total energy can be deduced with amplifiers having short and long shaping times, respectively. Secondly, the particle can be followed through its Bragg curve as a function of time using a flash ADC.

Fig. 6 shows results as obtained with a beam of 35 MeV/A ^{14}N delivered by the supercon-

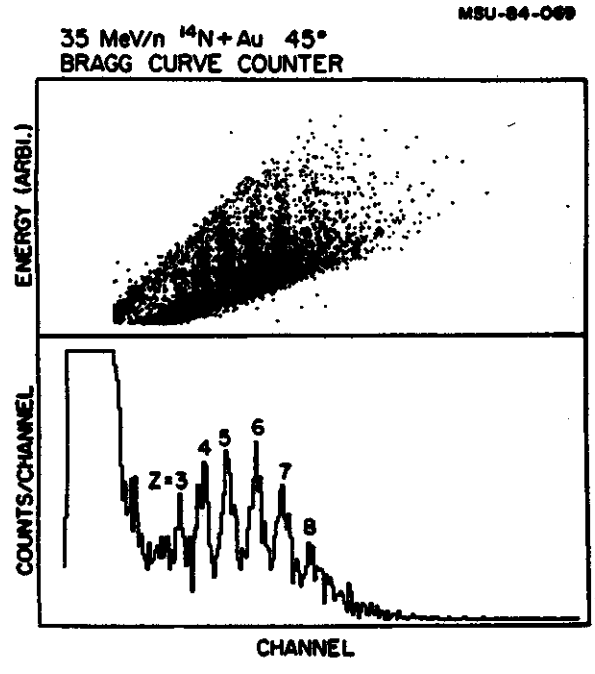

Fig.6 - Top: two-dimensional plot of Z (horizontal) versus E (vertical) for the reaction ^{14}N + ^{197}Au at 35 MeV/A.Bottom: projected Z spectrum for the same reaction.

ducting cyclotron of NSCL/MSU. Heavy fragments resulting from the reaction Au(^{14}N,X) were detected. The detector was placed at an angle of 45^0. The first (analog) readout method was used in this case. The anode signal of the BCC was, after amplification by a charge sensitive preamplifier, distributed to two spectroscopy amplifiers. One of these amplifiers was set at a time constant of 0.25 usec and therefore measures the charge Z of the ion; the other one was set at a timeconstant of 6 μsec and therefore measured the energy E. The top part of Fig. 6 shows a two-dimensional plot of the charge Z (horizontal axis) versus E (vertical axis). The bottom part of Fig. 6 shows the one-dimensional projection (Z-spectrum) of the same reaction. The charges are indicated. Another example obtained for higher charges is shown in Fig. 7. Results from the reaction ^{35}Cl + ^{58}Ni are presented. The beam of 230 MeV ^{35}Cl was provided by the Argonne tandem/linac accelerator. Charges up to Z=17 are observed in this case. In the two-dimensional Z versus E plots, the Z lines usually appear slightly curved, and more so near the "punch-through" line. Despite these effects, the individual charges remain resolved and can be isolated using two-dimensional contour gates. The spectra shown in the bottom of fig. 6 and in fig. 7 are not corrected for these nonlinearities. As an illustration of charge separation, we show in Fig. 8 energy spectra for Be,B and C fragments resulting from the reaction ^{12}C + ^{12}C at 30 MeV/nucleon. To obtain the energy calibration,

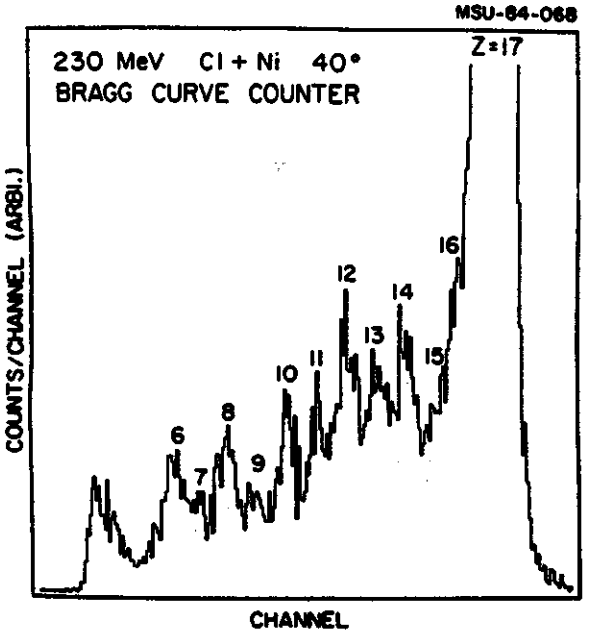

Fig.7 - Charge spectrum for the reaction ^{35}Cl + ^{58}Ni at 230 MeV.

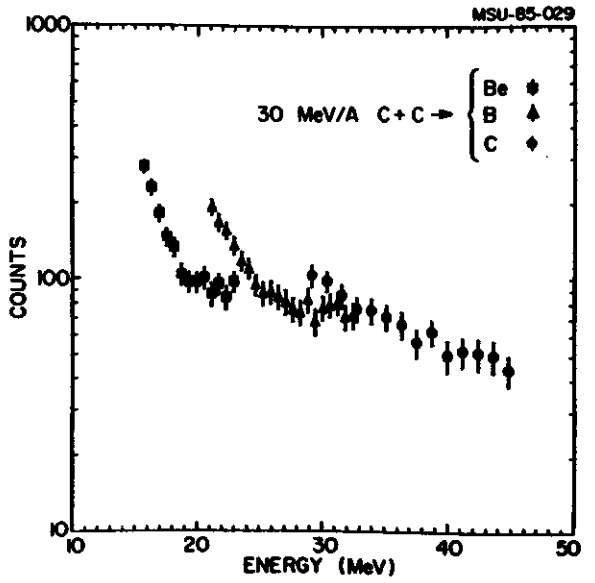

Fig.8 - Energy spectra for Be,B and C fragments from the reaction ^{12}C + ^{12}C at 30 MeV/A, as measured with the Bragg Curve detector.

we used the line which show up in the Z versus E plot and correspond to fragments that barely make it into the detector, and to fragments that punch through. The particles with energies in the vicinity of these extremes are excluded (with a software gate). This calibration is linear to a good approximation. The energy loss through the pressure windows is taken into account.

The current signal of the BCC for α particles from a ^{228}Th source is shown in Fig. 9. The signal was amplified by a timing filter amplifier. The Bragg curves for the two main α - lines (6.09 and 8.78 MeV) are clearly visible. The second method of reading out the BCC utilizes this current signal. This signal is digitized by a flash encoder that integrates the charge in 30 - 100 nsec time bins. Again, the

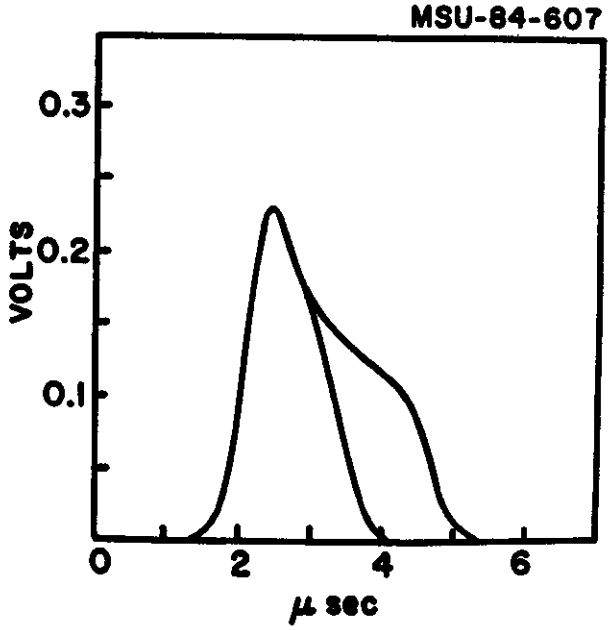

Fig.9 - Bragg curves for α - particles from a ^{228}Th source, as observed on an oscilloscope.

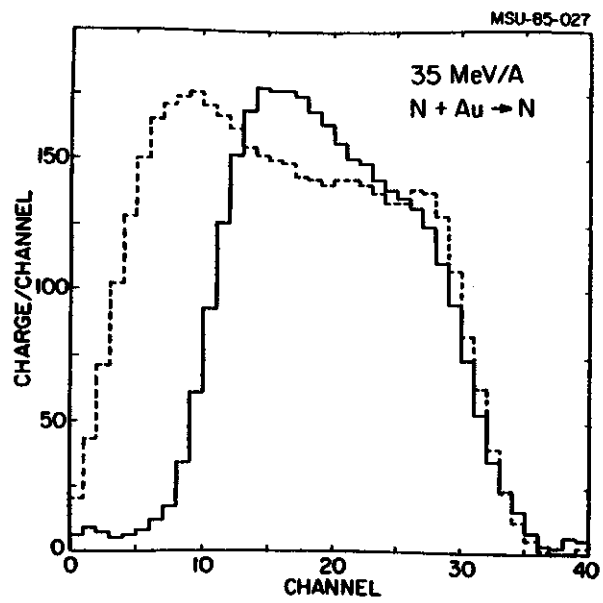

Fig.10 - "Snapshot" of the BCC, i.e. the digitized current output as measured with the flash encoder.

peak of the distribution can be related directly to the Z of the passing ion, and the integral of the curve is the total energy. Typical Bragg curves (snapshots), obtained this way for the reaction ^{14}N + Au at 35 MeV/nucleon, are shown in Fig. 10. The two curves shown correspond to N fragments of different energies. Note that the two curves show the same peak height (corresponding to Z) but different areas (corresponding to E). The X - axis of Fig. 10 corresponds to time; the time actually runs from right to left since the readout is done from the anode. The calibration is 90 ns/channel.

In conclusion, the test results reported here demonstrate the suitability of the prototype detectors for use as the basic building block of a 4π array. Construction of the final 4π array for use in phase 1.5 at NSCL is well underway.

---

a Department of Physics, University of Michigan, Ann Arbor, Michigan 48109
b Chalk River Nuclear Laboratory, Chalk River, Ontario K0J1J0, Canada

1. A.Breskin, Nucl.Instr.and Meth. 196,11(1982)
2. C.R.Gruhn et al., Nucl.Instr.and Meth. 196,33(1982)
3. H.H.Gutbrod et al., Nucl.Instr.and Meth. 203,189(1982)

S800 PROGRESS REPORT

A.F. Zeller and J.A. Nolen

Since the last report many of the large items which compromise the dipole magnets have been received. Formost has been the receipt of the dipole steel. The two 70 ton dipoles have been reassembled into their proper configurations to insure that no damage occured during shipping, and to measure the clearances with the bobbins in place. The pole tips assemblies were also leak checked.

The two stainless steel bobbins, into which the coils will be wound have also been received. They were cold shocked with liquid nitrogen and leak checked. All leaks have been repaired and the bobbins are now helium leak tight.

The superconducting wire has also arrived and some of it tested. Eight out of the thirteen lengths of conductor were tested at Fermi lab for their short sample current capabilities as a function of applied magnetic field. The required 1000 amps at 2T was exceeded in all samples. The measured currents at 2T were 1435 to 1695 amps at a criterion of 1μV/cm.

The dump resistors and dump switches are in house. The resistors are 0.5Ω and are designed to take the entire 1.1 megajoules of stored energy with only air cooling. The dump switches will break 500 amps at 250V in 0.1 sec. This value will limit the maximum temperature rise in any small segment of conductor in the event of a quench to 75°K if a dump is initiated within one second after a quench occurs. Even a ten second delay keeps the temperature rise below 200°K.

Design of the quadrupoles continues, but we are awaiting results from the prototype beamline quad to give us some feedback.

We are gratefull to Dr. A.D. McInturff of Fermi lab for doing the short sample measurements.

THE S320 SPECTROGRAPH

J. van der Plicht, S. Bricker, J. Yurkon

The S320 spectrograph, and the initial tests performed with beams from the K500 cyclotron are described in previous Annual Reports (1981-82 and 1982-83).

During the period which is covered in this Annual Report, the spectrograph was further optimized and used extensively in a variety of experiments. Typicaly, an energy resolution $\Delta E/E \sim 10^{-3}$ (linewidth around 1 mm) is obtained.

Experiments that were succesfully performed are:

- elastic scattering with ^{12}C beams of 15,25 and 35 MeV/A;
- inelastic scattering (giant resonances) with 35 MeV/A ^{6}Li and ^{14}N beams;
- heavy ion transfer reactions such as $(^{6}Li,d)$,$(^{6}Li,^{8}B)$,$(^{6}Li,^{6}He)$ and $(^{12}C,^{12}N)$;
- $(\alpha,^{3}He)$ and (α,t) studies at 100 MeV;
- mass measurements with the $(^{7}Li,^{8}He)$ and $(^{12}C,^{9}Li)$ reactions.

Several improvements on the instrument were implemented. The detection system has been changed in the sense that the stack of detectors now consist of a position sensitive single wire proportional counter in the focal plane, an ion chamber, the second ion chamber, the second single wire counter, and the 3" scintillator - in this order. The distance between the front - and back position sensitive wire counter is thus as large as possible, in order to obtain the best sensitivity for the angle of incidence of the particles which is directly calculated from these two position measurements.

In addition, the single wire counters have been modified. The wire has been moved to below the focal plane; the cathode foils carry a vertical driftfield. This way the measurement of the vertical position in the focal plane is improved, and the field shaping cathodes provide matching for the fields of the single wire counters and the ionchambers.

We constructed a monitor detection system consisting of 4 scintillators 0.125" thick NE102 with an active area of 0.25x0.25", equally spaced around the beam, approximately 6" after the target. They are individually coupled by means of flexible optical fiber light guides to Hamamatsu R647-01 miniphototubes. This setup allows for the detection of movements and asymmetries of the beam spot on target which is very important for elastic scattering experiments.

The scattering chamber has been upgraded to allow the top cover to remain stationary with respect to the beam while the spectrograph rotates. The monitor detectors are mounted on this cover plate. A new retractable, watercooled faradaycup will also be attached to the cover plate. This cover also accomodates the upgraded target transfer mechanism. Targets now can be transferred from targetlab to the S320 and back without breaking vacuum.

A retractable viewing plate was installed in the beam viewing box just in front of the focal plane. It can be set in 3 positions: out (for normal datataking), calibration mask (this is a tantalum plate with horizontal and vertical slots), and a watercooled beamstop with scintillators for direct viewing of the beam at 0 degrees.

To the dipole vacuum vessel, a viewing port at 0 degrees was added to ease alignment of targets, collimators and detectors significantly. A roughing line system was installed so that separate parts of the spectrograph can be pumped down separately from one pumping location with vacuum interlocked valves. Interlocks were added to the spectrograph carriage drive to set

limits (positive and negative) on the carriage travel. Also, an extra patch panel was added above the wedge to ease cabling for detectors etc. in that area.

A low pressure Multiwire Proportional Counter (MWPC) was built. We found however that the gain for this type of detectors was marginal for a typical beam of say 35 MeV/A ^{14}N particles. We are presently upgrading this detector to a "Multistep Detector" by adding additional multiplication stages. This detector will be mounted at the end of the wedge, just in front of the apertures. It is position sensitive in 2 dimensions.

The computerprogram to be used for calculations of fieldsettings has been improved considerably. It can calculate energy losses, time of flight and scintillator light, of ions and charge states in the focal plane detectors. It produces two dimensional plots, which are very usefull for particle identification purposes. The energy loss calculations are based on the formulas from Ziegler's handbook of stopping powers.

An extensive Users Manual was written in order to assist outside users setting up and running their experiments.

---

1. J. Speth and A. van der Woude, Rep. Prog. Phys. 44,719(1981).
2. C.K. Gelbke, Giant Multipole Resonance Topical Conference, Oak Ridge 1979.

THE NEUTRON FACILITY

B. Remington, G. Caskey, A. Galonsky, J. Kasagi[a], A. Kiss[b] and Z. Seres[b]

The neutron facility at NSCL has been operative now since May, 1983 and has been used in several "neutron experiments". The main components, which will be discussed in more detail below, are a quadrupole magnet at the exit of the S320 spectrometer for final focusing of the beam onto the target, a thin-walled scattering chamber designed for minimal neutron attenuation, and an extensively shielded beam dump about 12 ft downstream from the target (see Fig. 1).

For bringing a well-focused beam spot onto the target, a quadrupole focusing magnet is utilized. The quadrupole is located at the exit of the S320 spectrometer and is about 4.5 ft from the target at the center of the chamber. This provides a final element of focusing and allows beam spots of < 1/4" diameter. To reduce the possibility of beam striking solid-state detectors at forward angles, two collimators (1.5" and 1" apertures) are placed about 1 ft apart in the beam line just before the entrance to the chamber. The collimators are electrically insulated from the beam line to allow charge collection in the case of off-center beams. The net result is that the beam can be well positioned and focused at the center of the neutron chamber. Another shield can be placed to the sides of the target ladder. The combination of collimators and target-ladder shields provides adequate protection for even very forward angle detectors from stray beam.

The chamber, (see Fig. 1) which was obtained from the University of Rochester in ~1965, served as the first scattering chamber for the M.S.U. K50 cyclotron. It is made out of 1/8" steel, has a 36" diameter, and a target drive, which can be operated from inside the vault or from the data acquisition area, is mounted on the top port (6" diameter). The target drive extension is calibrated in millimeters and can be read off digital displays both in the vault and from the data acquisition area. The target ladder can also be rotated without breaking vacuum, but this must be done manually.

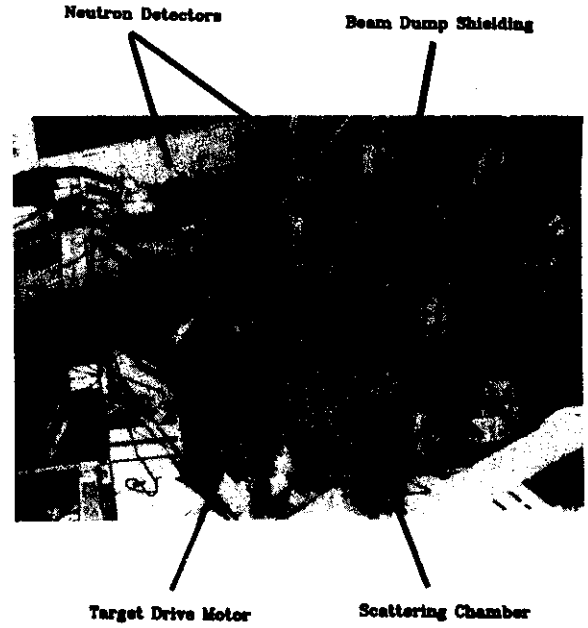

Fig. 1 The neutron chamber as viewed from above. The beam enters the chamber through the entrance flange, shown in the foreground (bottom of the picture), and exits into the beam dump, shown in the background (top of the picture). One also can see typical placement of neutron detectors around the chamber in neutron TOF measurements.

Features exist for mounting detectors inside the chamber. Ideal for silicon telescopes are a pair of low-mass, circular-sector plates, upon each of which can be mounted comfortably 3 silicon telescopes (see Fig. 2). These plates can be separately positioned (manually) and are equipped with cooling lines to allow for cooling of the telescopes by circulating refrigerated methanol. A third smaller plate can be mounted at various polar angles out of the horizontal plane below the beam.

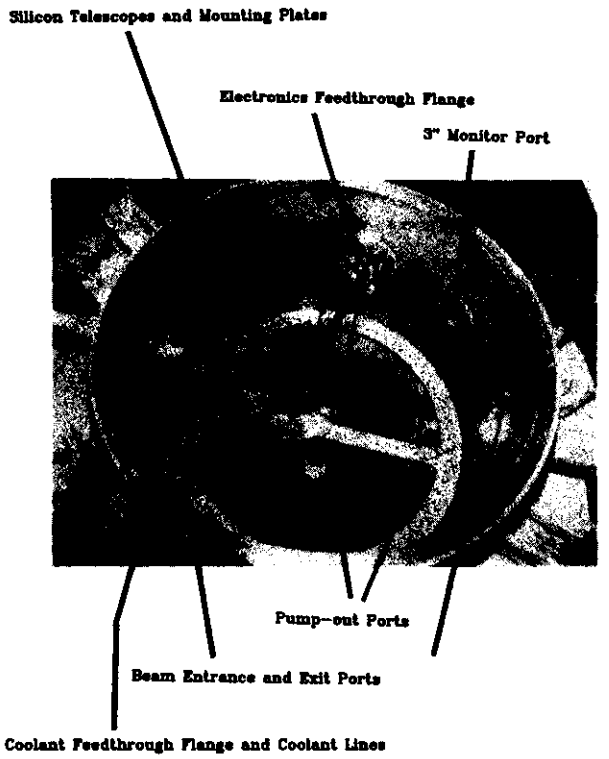

Fig. 2 The inside of the chamber showing the solid state telescope mounting plates, along with the cooling lines and coolant feedthrough flange (lower left) and the electronics feedthrough flange (top of photograph).

There are two pumpout ports on the chamber, one a 1" rough-out port fitted with a KF-40 fitting, and the other the main 9" port at the bottom to which a CRYO-TORR 7 pump gets mounted (see Fig. 2). There are four large ports on the walls of the chamber, two of which constitute the entrance (6" ID) and exit (7" ID) ports for the beam. A third (6" ID) is typically used as the electronics feedthrough, using a black lexan flange fitted with 20 feedthroughs, 15 of which are BNC, and the remainder SHV. The remaining 6" port has typically been covered with a clear lucite flange and used for visual monitoring of the orientation of the targets and detectors inside the chamber. There are two smaller 3" ID ports. One is typically fitted with a clear lexan flange and used to remotely monitor with a camera the beam spot on an Al_2O_3 scintillator mounted on the target ladder. The second can be fitted with a black lexan flange housing the coolant feedthroughs (see Fig. 2).

The exit beam line extends about 12 feet to where the beam is deposited on 1" of 1100 grade Al backed by a 1/2" thick brass plate containing fitted copper cooling lines. In one possible configuration, this entire stretch of beam line is 6" ID, 1/4" wall Al, including a 6" bellows and "T" that can be rigged with a plunger/scintillator-camera arrangement to allow monitoring of the beam at the entrance to the beam dump (see Figs. 1 and 3). In another possible configuration, a section of the 6" beam line is removed and replaced with a section of reduced-mass 4" beam line. This is useful for experiments where neutrons are going to be

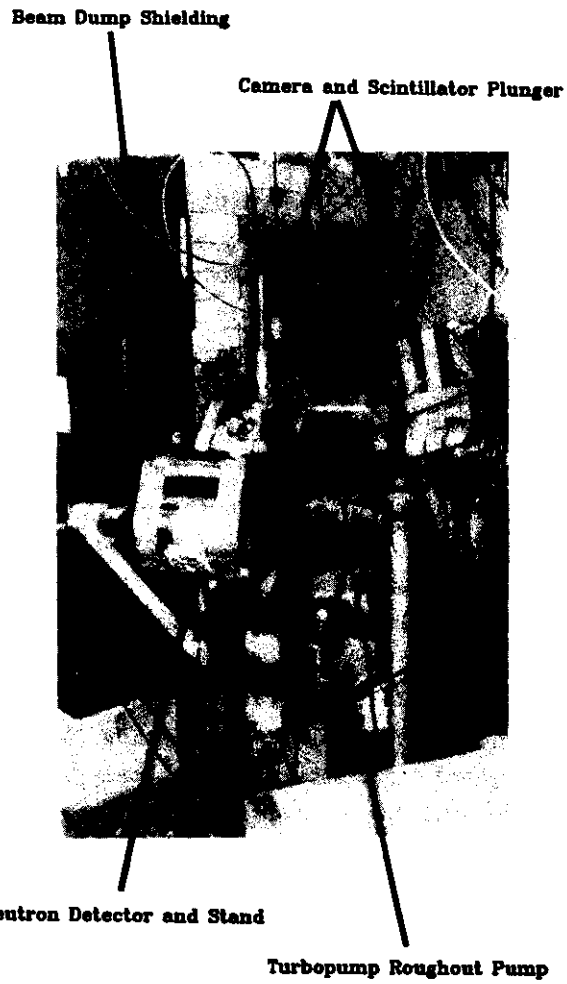

Fig. 3 The 6" exit beam line as it enters the extensively shielded beam dump. Also shown are the plunger/camera arrangement for monitoring the beam just prior to entering the beam dump and one of the neutron detector stands.

detected at angles of 10° or less. Fig. 4 shows the calculated attenuation of neutrons detected at 10° as a function of neutron energy.[1] The solid line is for the reduced-mass 4" exit beam line section and after the exit port ID had been enlarged from 6" to 7". The circles are for the 6" exit beam line section for the original 6" ID exit port (i.e., before it had been enlarged). Reducing the amount of material between the target and the detector gives a substantial reduction in the attenuation of neutrons.

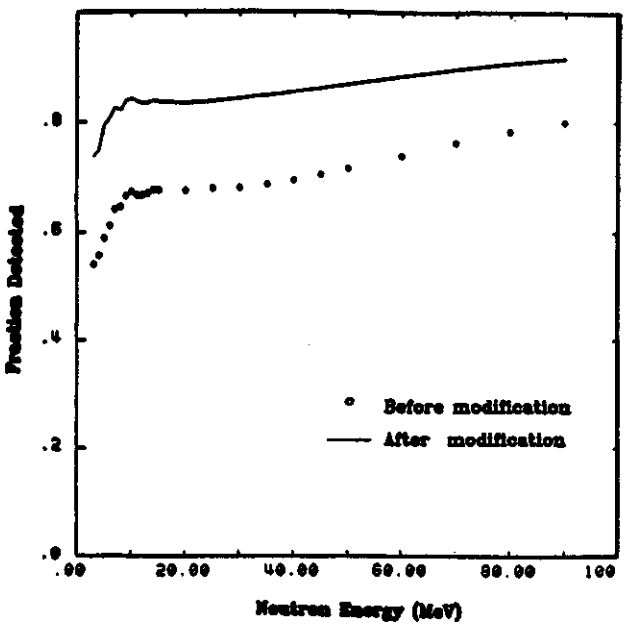

Fig. 4 Attenuation calculations before and after modification of the exit port and beam line to reduce the amount of material between the target (located at the center of the chamber) and a neutron detector outside the chamber at an angle of 10°.

The main features of the beam dump are an electrically insulated Faraday cup to allow charge collection and extensive shielding around it to prevent the radiation produced when the beam is stopped from entering nearby neutron detectors. The main element of shielding is provided by two 18" thick steel slabs, each weighing over 20,000 lbs (originally the yokes of the famous 40" U of M cyclotron magnet used in the 1930's and 1940's). The remainder of space is filled in with concrete blocks and lead bricks (see Fig. 3). The effectiveness of the shielding is illustrated by the fact that neutron detectors have been operated near the entrance to the beam dump, as can be seen in Fig. 3. Fig. 5 shows a TOF spectrum taken with the detector pictured in Fig. 3, with the level of background indicated by triangles. As one can see, the background in this potentially bad configuration is typically less than ~10%, with much of this coming from scattering from the floor.

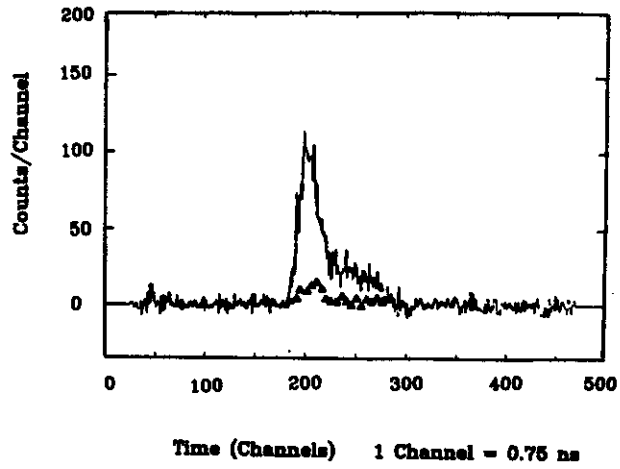

Fig. 5 A typical neutron TOF spectrum for θ_n = 10° showing both the "raw" counts (histogram) and that contribution due to background neutrons (triangles).

The Faraday cup consists of a 7 ft long section of 6" beam line insulated by 20 mil of mylar from a rolled and riveted 14 gauge steel shell. In principle, the Faraday cup is removable from this steel shell, which is fixed between the steel slabs of the beam dump with poured concrete and concrete blocks. The ability exists to cool the Faraday cup by circulating deionized water or forced air, but for present beam intensities and energies (eg., 40 ena of 35 MeV/A ^{14}N) this has not been necessary.

In Fig. 3 one also can see the turbopump that is used as the second stage of the pumpdown. Typical pumpdown procedures are as follows: Roughing is initiated with both the mechanical pump attached directly to the chamber

and through the roughing pump attached to the turbopump. Then the mechanical pump at the chamber is valved off, and the turbo pump is started. Roughing continues via the turbopump until the vacuum in the chamber is 50-100 mTorr, at which time the turbo is valved off and the valve to the cryopump is opened. Pressures of $\sim 1 \times 10^{-5}$ Torr are readily attainable and satisfactory for typical heavy-ion experiments. A note of caution: once the turbopump is valved off, either it should continue to pump, or both it and its mechanical pump should be turned off (such that they automatically vent). One should **NOT** turn off the turbopump while allowing its mechanical forepump to continue pumping. The vapor pressure of the forepump oil is sufficiently high that the beam line may be at risk of contamination when the turbopump is not running, and hence, not acting as a baffle against backstreaming of oil. One immediate consequence of such a scenario is that this backstreaming oil could find its way down to the cold heads of the cryopump, causing excessive loading on the pump or possibly even a shutdown to regenerate the cold heads. The temperature of the cryopump should be monitored during the course of an experiment, and should remain below 25 °K for normal operating (green or yellow-green on the LED thermometer).

As can be seen in Figs. 1-3, there exist ten neutron detector stands, ten 12" by 3" brass cylinder shadow bars, ten wooden mounts to hold the shadow bars, and three wooden tables that fit around the chamber to allow for placement of shadow bars, preamps, etc.

Bringing the neutron line into operation took the efforts of people from many different departments across the lab, including the Departments of Nuclear Physics, Mechanical Design, Electrical Design, Machine Shop, and Operations. Special thanks are offered to Len Morris of Mechanical Design for his role in designing and supervising the construction of the hardware of the neutron line.

---

a. Tokyo Instityte of Technology, Tokyo, Japan
b. Eötvös University and CRI Institute of Science, Budapest, Hungary

1. B. Remington, Doctoral Thesis, MSU Physics Dept., expected June 1985

VACUUM SYSTEM OPERATING EXPERIENCE FOR BEAMLINES AND EXPERIMENTAL CHAMBERS

A.D. Waddell and R.A. Blue

Three types of pumps are utilized for high vacuum service on beamlines and experimental chambers. The beamline vacuum is maintained by the combination of two cryopumps and six triode ion pumps. Experimental chambers are pumped primarily by cryopumps, assisted in some cases by turbomolecular pumps. Several mobile turbopump systems which can be easily moved about are available for use on an "as needed" basis throughout the laboratory. If, for example, the beamline has been vented for service, a turbopump will be used for the initial pumpdown.

A major portion of the cryopump maintenance is the cleaning of oil-contaminated pumping arrays. Of the different cleaning techniques we have tried the best seem to be cleaning the first stage array and radiation shield with Alconox laboratory detergent and ultrasonically cleaning the second stage array using Freon TF, followed by a vacuum baking cycle. Depending on the degree of oil contamination, the charcoal array is run through either one or two ultrasonic cleaning cycles. If the array is badly contaminated, we start with previously used TF for an initial degreasing, followed by a cycle using fresh TF. Both cleaning cycles are run for about fifteen minutes after the solvent has begun cavitation. The array is then vacuum-baked at 100 millitorr and ~130 degrees F overnight to drive the Freon from the charcoal. It is important not to exceed 150 degrees F when baking as the epoxy that holds the charcoal to the inner surface of the array may break down. After approximately 8 hours of baking, the heater is turned off; when the temperature has returned to room temperature, the oven is backfilled with dry nitrogen and pumped out three times. After a final nitrogen backfill, the array is removed from the oven and placed in Ziploc plastic bags with desiccant cartridges until ready for use. These procedures seem to restore the pump capacity adequately for our needs, though no testing has been done to determine exactly how much capacity has been regained.

The source of the oil responsible for cryopump contamination is generally a mechanical pump employed in rough pumping the system. Our recommended procedures call for a restriction in the use of such pumps to the pressure range above 100 millitorr where, it is thought, oil backstreaming is not significant. We expect to investigate this problem further to determine whether a higher roughing cutoff or a more rigid enforcement of the 100 millitorr limit is required.

The most routine maintenance required for cryopumps is periodic regeneration of the pumping arrays. We have experimented with a number of different procedures to speed up and/or more thoroughly regenerate the cryos. A dry nitrogen backfill (preferably heated, to not more than 130 degrees F) has proven extremely helpful in shortening the time required to rough and restart the pump. The backfill is started immediately after the pump is shut down, when the ice on the first stage array still has a large surface area, allowing a great volume of the pumped water vapor to move into the dry nitrogen and out of the pump. The nitrogen flow is continued for 15-30 minutes after the pump has reached room temperature. The cryo is then roughed to 50 millitorr (and no lower) and is valved off from the roughing line. A rate-of-rise test is then used on the cryopump, with 10 millitorr/minute or less deemed acceptable. If the rate of rise is larger the backfill is continued for another 5-10 minutes. An alternate method being tried that may prove more useful is to rough pump the cryo while flowing nitrogen into it at a rate that keeps the pressure inside the cryo at ~500 millitorr. This may increase the amount of water removed

from the pump using nitrogen backfilling alone, as the water-saturated nitrogen is immediately removed from the inside of the cryopump vacuum space. This procedure is done after bringing the pump up to room temperature using the backfill procedure described above. We have found it necessary to check the pressure relief valve on the cryopump for cleanliness since we began using these procedures, as small particles of dirt or dust from inside the cryo vacuum space can be blown out of the relief port as the nitrogen flows, preventing the valve from resealing. This has proved to be a minor concern and is easily remedied.

Major rebuilding of cryopump coldheads has been done in-house. This involved the purchase of special tools and support equipment, and also the development and maintenance of a spare parts inventory. We currently are using (7) CTI CT7 pumps, (4) CTI CT100's, and (4) Varian VK12C cryopumps. The cost for a complete rebuild of a well-worn CTI coldhead is approximately $450 for parts and 8 man-hours of labor. Often, though, some parts do not need replacement so the cost is lower. Also, this rebuilding requires a skilled technician, though the routine maintenance can be done by a relatively unskilled person.

With respect to operation, reliability, and routine or major maintenance, the CTI's have proved to be our preferred pumps. For example, removal of the first stage array for cleaning or access to the second stage array involves removing 6 easily accessible screws on the CTI's, while the Varians use 20 screw/nut sets which are somewhat difficult to reach. In major rebuilding the CTI's, though they contain more parts, are easier and more straightforward to service. An example is replacing the displacer seals: the CTI has two ready-to-use Teflon seals, while the Varian has eight Teflon crescent-ring seals which must individually be carefully dressed to fit before installation, using very fine sandpaper and a surface plate. Also, we have had numerous compressor problems with the Varians, with two of them returned for factory repair. The CTI compressors have been very reliable, durable, and easy to maintain. In short, the CTI systems are easy to use, maintain, and rebuild. They are also more predictable and reliable than are the Varian VK12C systems.

Except where the large pumping speed of a cryopump is required, turbomolecular pumps are favored in most of our applications. We now have four Leybold-Heraeus 150 l/s mobile turbomolecular pump units. They have been quite reliable, apart from a few easily repaired problems, and are also quite durable. We have continued to have problems with our Alcatel mobile turbo unit which have been multiplied by the lack of parts, information, and service support from the company. We have just received a Sargent-Welch 280 l/s turbopump for use on our 60" scattering chamber. It has performed well to date.

Our Thermionics 60 l/s triode sputter-ion pumps continue to perform well, with just two pumps requiring service in 3 years continuous operation.

We purchased six Edwards E2M8 direct-drive mechanical pumps this year, and have found them to be reliable and durable. One pump developed a locked rotor after a month or two of service and was returned under warranty for factory repair. It has done well since it was returned to service.

In general, our vacuum systems have performed well, requiring not much more than routine inspection and service. A large number of problems (with the exception of oil contamination) can be diminished or eliminated by daily inspection of each system's operating parameters. We now have used such an inspection routine for over a year, and have found it invaluable in spotting immediate and future problems with our systems, making consistent system performance and convienient service times more easy to attain.